Current Biology, Volume *27*

Supplemental Information

Responses to Spatial Contrast in the Mouse Suprachiasmatic Nuclei

Joshua W. Mouland, Adam R. Stinchcombe, Daniel B. Forger, Timothy M. Brown, and Robert J. Lucas

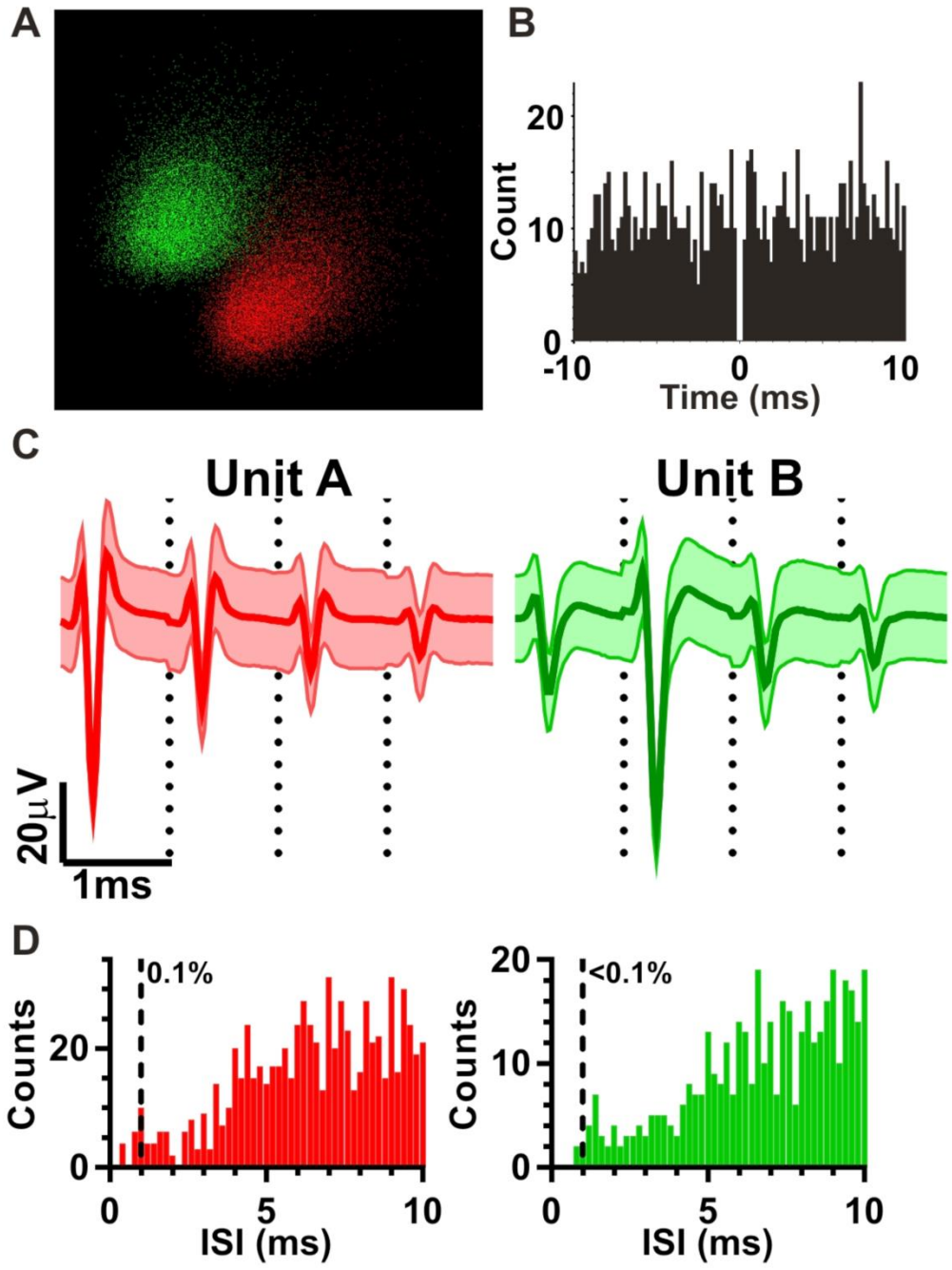

Figure S1: Spike sorting Validation. Related to Figures 1-3. A-D. Show two single units that were located on the same tetrode (unit A in red and unit B in green). **A.** The two units separated using principle component analysis and waveform parameters. Here peak to trough amplitude on electrode site one and two respectively. **B.** Crosscorrelogram of unit A vs unit B (bin size =0.2 ms). **C.** The tetrode waveform for each unit (mean±s.d.). Each tetrode waveform is comprised of the waveform at a given epoch across four electrode sites. The dotted line denotes the start of the epoch for each electrode. **D.** Interspike interval for each unit (0.2 ms bins). The dashed black line denotes the percentage of spikes that fall within 1ms of another spike.

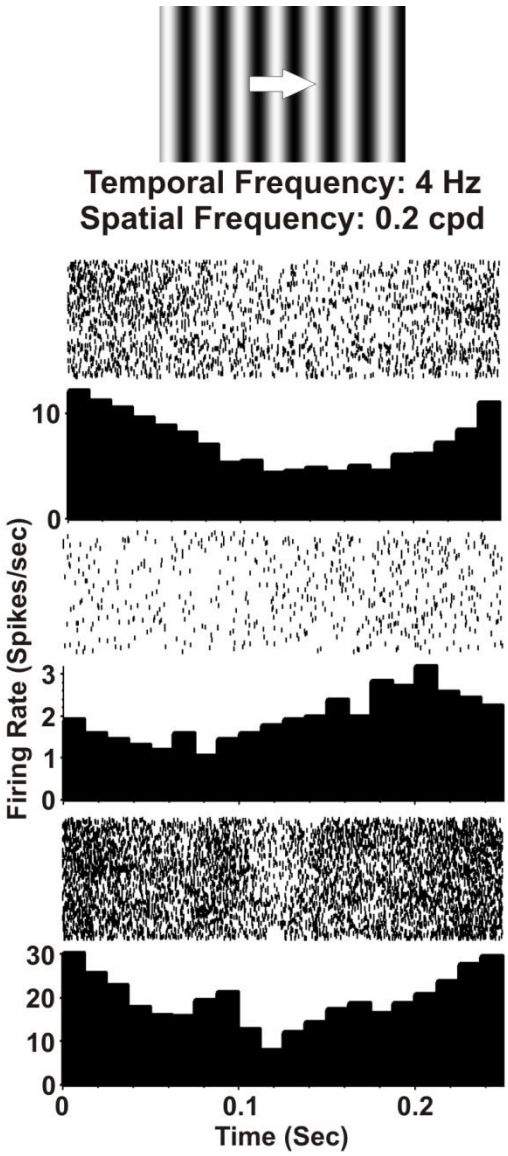

Figure S2: Single units tracking drifting gratings at 0.2cpd. Related to Figure 2. Perievent histogram (above) and raster plots (below) of spike firing (12.5 ms bins) from three single units that showed significant modulation (as determined by spectral power analysis) by a drifting sinusoidal grating at 0.2cpd (1200 repeats at 4Hz).

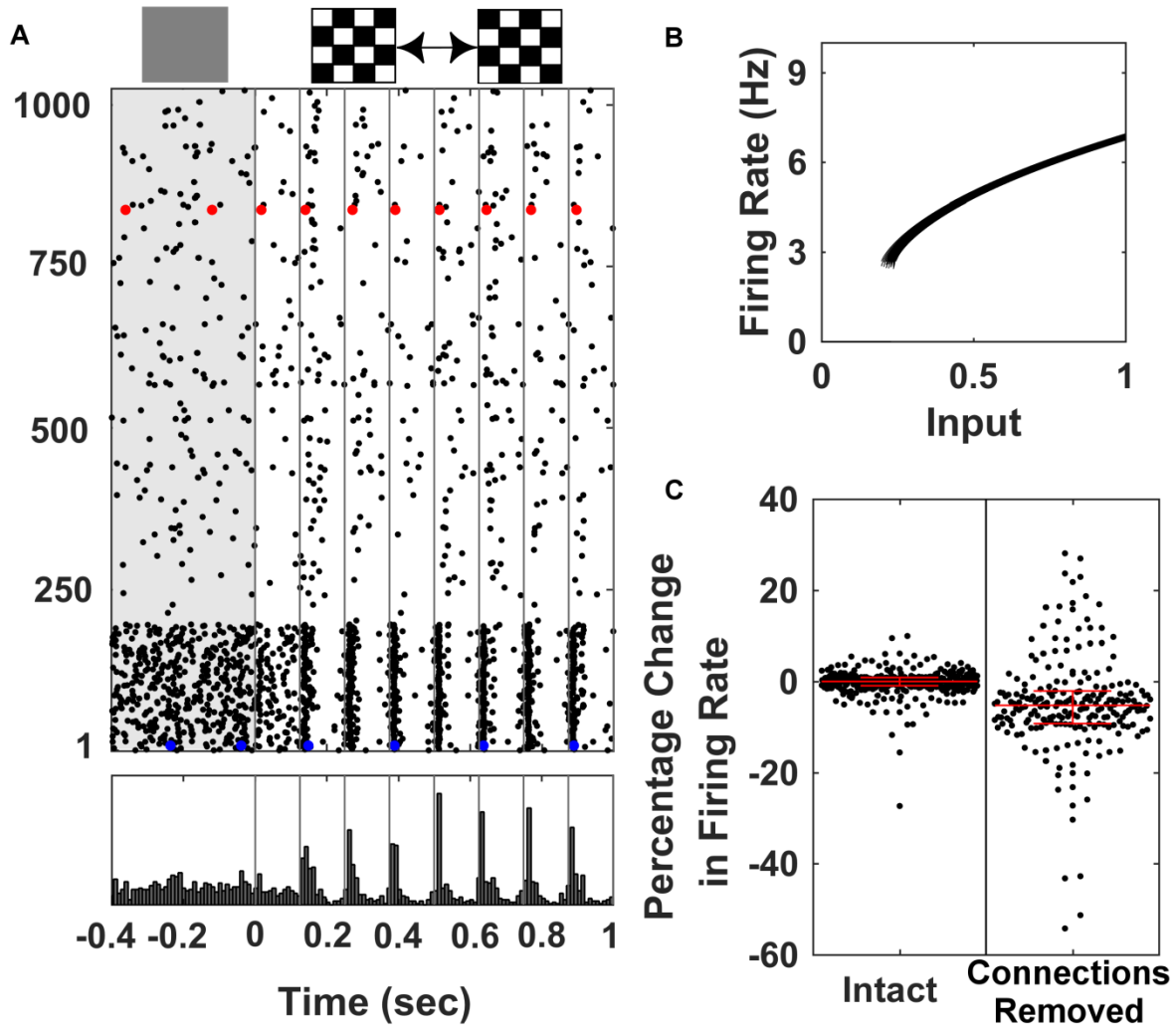

Figure S3: A simulation of the electrical activity of the SCN. Related to Figure 3. The membrane voltage of each of 1024 neurones evolve according to a conductance-based model that incorporates sodium, potassium, and calcium currents and has been fit previously to extensive electrophysiology experiments[S1-4]. Each SCN neurone receives synaptic input from other SCN neurons, while a subset of the SCN neurons receive input from a 14 by 14 array of ipRGCs whose receptive fields tile a detail of the visual scene. The connectivity within the SCN and from the retina to the SCN has been selected as to reproduce the range and proportions of the spatial RFs described in this manuscript. **A**. Raster plots of activity (dots represent spikes) over 0.4 second uniform illumination (shaded grey) followed by 1 sec exposure to a 4Hz inverting 14 by 14 chequerboard stimulus. Each stimulus inversion is denoted with a grey vertical line. Below the raster is a histogram of the spike times for the neurones with a bin width of 10ms. Note the widespread 4Hz periodicity in firing (the neurone with blue dots for example) and in some cases frequency doubling (the neurone with red dots for example) that has been observed experimentally. The spatially patterned input affects the timing of spikes for many neurones. **B.** The input-output relation of a single model SCN neurone. The steady firing rate of a model neurone is plotted as a function of constant input for each circadian time at which

experimental data was collected. They show a uniform input threshold to generate firing and a saturating of the firing rate for large inputs. According to this input-output relation, we expect that an individual neurone could have either a higher or lower firing rate for patterned input over uniform illumination depending on its retinal and SCN network inputs. **C.** Distribution of changes in firing rates of 381 (Intact) and 222 (Connections Removed) simulated spiking SCN neurones from a uniform grey condition to a 4Hz inverting 14 by 14 chequerboard stimulus (100% x (FRinverting chequerboard - FRUniform)/FRUniform; median and interquartile range shown in red). Both increases and decreases in the firing rates are observed, matching experimental data in Figure 3C. The network within the SCN acts to attenuate the overall impact of contrast since after removing these connections the SCN neurones show a greater spread in firing rate in response to the patterned stimulus.

Supplemental References

[S1] Diekman, C.O., and Forger, D.B. (2009). Clustering Predicted by an Electrophysiological Model of the Suprachiasmatic Nucleus. J. Biol. Rhythms *24*, 322–333.

[S2] Diekman, C.O., Belle, M.D.C., Irwin, R.P., Allen, C.N., Piggins, H.D., and Forger, D.B. (2013). Causes and Consequences of Hyperexcitation in Central Clock Neurons. PLoS Comput. Biol. *9*, e1003196.

[S3] DeWoskin, D., Myung, J., Belle, M.D.C., Piggins, H.D., Takumi, T., and Forger, D.B. (2015). Distinct roles for GABA across multiple timescales in mammalian circadian timekeeping. Proc. Natl. Acad. Sci. *112*, E3911–E3919. Available at: http://www.pnas.org/lookup/doi/10.1073/pnas.1420753112.

[S4] Dewoskin, D., Geng, W., Stinchcombe, A.R., and Forger, D.B. (2014). It is not the parts , but how they interact that determines the behaviour of circadian rhythms across scales and organisms. Interface Focus *4*, 20130076.